DINAME 2017 - Proceedings of the XVII International Symposium on Dynamic Problems of Mechanics
A. T. Fleury, D. A. Rade, P. R. G. Kurka (Editors), ABCM, São Sebastião, SP, Brazil, March 5-10, 2017

AEROELASTIC RESPONSE OF SHAPE MEMORY ALLOY HYBRID COMPOSITE CYLINDRICAL SHELLS UNDER SUPERSONIC FLOW

Alfredo R. de Faria[1], **Maurício V. Donadon**[2]

[1] Instituto Tecnológico de Aeronáutica, Dept. of Mechanical Engineering, São José dos Campos, arfaria@ita.br
[2] Instituto Tecnológico de Aeronáutica, Dept. of Aeronautical Engineering, São José dos Campos, donadon@ita.br

Abstract: Shape Memory Alloy Hybrid Composite (SMAHC) laminates are built with continuous carbon fibers and Shape Memory Alloy (SMA) wires, both embedded in a polymeric matrix thereby forming a three constituent composite material. The SMA actuation is triggered by temperature changes, resulting in modifications in the structural responses of SMAHC laminates. A particularly important structural characteristic of SMAHC laminates which is investigated in this paper is the aeroelastic stability boundary of flutter. The derivation of the effective mechanical properties of the SMAHC is based on micromechanical model which accounts for temperature and fraction of martensite/austenite transformation phases of the shape memory alloy. The mathematical problem is formulated using Hamilton's principle, allowing for derivation of the equilibrium equations and boundary conditions of the aeroelastic response. The governing equations are then discretized and solved by the finite element method. A parametric study is conducted where different geometric configurations, laminate stacking sequence, boundary conditions and curvatures are investigated. It is observed that the SMAHC structure is stabilized against flutter by proper tailoring of stiffening effects induced by the changes in the fraction of martensite/austenite transformation phases of the SMA. Therefore, it is possible to increase critical flutter speed by controlling the temperature of the SMA wires.

Keywords: aeroelasticity, flutter, composites, shape memory alloy

INTRODUCTION

The volume of research devoted in recent years to shape memory alloys (SMA) led scientists and engineers to gain critical knowledge about these versatile materials. Nowadays, accurate models describing the thermomechanical behavior of SMA allows one to use them in practical engineering applications. In most cases the phase transformation from martensite to austenite or vice-versa is achieved through the Joule effect where electrical current generates heat required to induce the phase transformation.

In the aerospace sector SMA can be used in a number of situations. An important aspect of this type of alloys is their slow response time. Usually the phase transformation takes relatively long, what renders them useless in applications where time is crucial, e.g., in active control of flexible structures. In this case the use of a network of piezoelectric actuators is recommended (Faria and Almeida, 1997). However, SMA have extremely large authority when compared to piezoelectric actuators, i.e., they are able to exert large forces and moments. This particular feature makes SMA suitable for applications such as morphing and stress stiffening. For instance, natural frequencies and flutter speeds of composite panels can be increased via the actuation of SMA.

One of the earliest works on the use of SMA to modify flutter characteristics of composite plates is the paper by Parka *et al.* (2005). Composite plates embedded with SMA wires are considered. The laminate is assumed to be composed of conventional composite layers (fibers + resin) and SMA layers composed of resin and SAM wires in lieu of conventional fibers. A micromechanics approach is used to obtain the constitutive equations of the SMA layers. A FSDT plate model is used to formulate the FE governing equations. The authors demonstrated that both natural frequencies and flutter speeds could be modified through actuation of SMA fibers.

Guo *et al.* (2007) derived a finite element nonlinear model to investigate supersonic flutter of composite plates. The quasi-steady first-order piston theory was the aerodynamic model selected to describe the aerodynamics pressure over the panel. Similarly to Parka *et al.* (2005), the authors considered two types of layers: conventional composite layers and SMA fiber reinforced layers. It was shown that the introduction of SMA layers into the laminate substantially improved the response of the SMAHC plates.

SMAHC curved panels were first studied by Ibrahim *et al.* (2009). The authors employed the Marguerre curved-plate theory to investigate flutter of composite panels at elevated temperature. First-order quasi-steady piston theory is used again to model the supersonic flow state. It was concluded that SMAHC panels can efficiently control flutter at elevated temperatures by increasing flutter boundaries when compared to traditional composite laminates.

The work by Kuo *et al.* (2012) also uses a micromechanical approach to obtain the effective engineering constants of a SMA layer. The thermal effects are assumed to be restricted to the SMA fibers. Cross-ply and angle-ply laminates were investigated having one SAM layer in the middle of the laminate. Flutter boundaries were obtained for different volume fractions of SMA fibers in the SAM layers. Not surprisingly, it was shown that the higher the volume fraction content of SMA layers, the more effective is the flutter control.

In the studies published up to now layers of the laminates are assumed to be made of traditional fiber/resin or SMA/resin. However, there is no model that is capable of modeling layers where fiber/SMA/resin coexist simultaneously. The present paper brings forward a new micromechanical model where layers composed of three constituents are allowed: traditional carbon fibers, SMA wire and resin. Their volume fractions can be adjusted to represent different proportions of the three constituents. From a practical point of view volume fraction of the resin cannot be smaller than 50%, or fabrication of real laminates would not be feasible. The numerical solution of the governing equations is achieved by the use of the finite element method where the R16 element (Bismarck-Nasr, 1991) is employed. This element maintains C1 continuity in between elements, what guarantees very high convergence rates, i.e., relatively coarse meshes already deliver very accurate results.

MICROMECHANICAL MODEL FORMULATION FOR THE SMACH LAMINA

Consider the representative volume element depicted in Fig. 1 composed by three different constituents named carbon fiber, SMA wire and resin representing a smallest repetitive unit cell of an unidirectional lamina. The lamina is assumed to be initially stress-free, linearly elastic. The reinforcements (carbon fiber and SMA wire) and matrix (resin) are assumed to be homogeneous, linearly elastic and isotropic. An ideal adhesion between reinforcements and matrix is also assumed. By using the mechanical of materials approach, the homogenized mechanical properties of the lamina can be obtained in terms of the constituents volume fractions (Kuo *et al.*, 2012; Kaw, 2006) as follows,

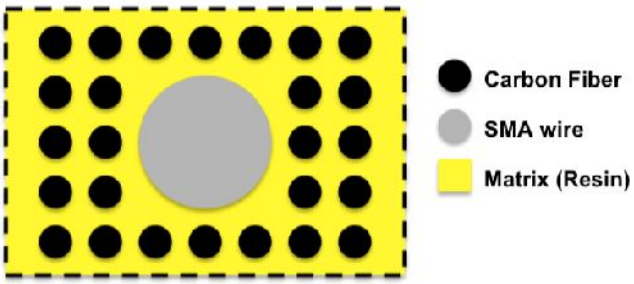

Figure 1 – Representative volume element of the SMAHC.

$$E_1(\xi,T) = E_f V_f + E_{SMA}(\xi,T) V_{SMA} + E_m V_m \tag{1}$$

$$E_2(\xi,T) = \frac{E_f E_{SMA}(\xi,T) E_m}{E_m E_{SMA} V_f + E_f E_{SMA}(\xi,T) V_m + E_f E_m V_{SMA}} \tag{2}$$

$$G_{12}(\xi,T) = \frac{G_f G_{SMA}(\xi,T) G_m}{G_m G_{SMA} V_f + G_f G_{SMA}(\xi,T) V_m + G_f G_m V_{SMA}} \tag{3}$$

$$\nu_{12} = \nu_f V_f + \nu_{SMA} V_{SMA} + \nu_m V_m \tag{4}$$

where E_1, E_2, G_{12} and ν_{12} are the longitudinal Young's modulus, transverse Young's modulus, in-plane shear modulus and Poisson's ratio, respectively, expressed in the material local coordinate system 123. E_f , E_m, $E_{SMA}(\xi,T)$ are the carbon fiber, matrix and shape memory alloy Young's modulus, respectively. V_f , V_m, V_{SMA} are the constituents volume fractions.

The proposed expressions for $E_{SMA}(\xi,T)$ and $G_{SMA}(\xi,T)$ are based on the SMA spring models available in the open literature Aquino *et al.* (2007),

$$E_{SMA}(\xi,T) = E_{\min} + \frac{\exp(\xi)(E_{\max} - E_{\min})}{1+\exp(\xi)} \tag{5}$$

$$\xi = \frac{\beta}{A_F - A_S}\left(T - \frac{A_F - A_S}{2}\right) \tag{6}$$

$$G_{SMA}(\xi,T)=\frac{E_{SMA}(\xi,T)}{2(1-\nu_{SMA})} \tag{7}$$

$E_{\min}$ and $E_{\max}$ are the maximum and minimum Young's modulus defined within the austenite temperature transformation range A_S and A_F. A_S and A_F are the initial and final temperatures associated with the material phase transformation. β is also a material constant related to the rate of austenite transformation. T is operating temperature of the SMA wire. Figure 2 shows the effects of temperature and SMA volume fractions on the the normalized modulus E_1/E_f. The SMAHC is made of a 3 mm thick AS4/8552 Carbon-Epoxy UD layer with embedded NiTi SMA wires. Due to manufacturing constraints, the resin volume fraction was kept fixed and equal to 50% in a such way that only the reinforcements (carbon fiber and SMA wires) volume fractions are allowed to change. The mechanical properties of the constituents are presented in Tab. 1.

Table 1 – Mechanical properties of the SMAHC constituents.

	Nitinol wire		Carbon fiber		Epoxy
E_{SMA}	30 GPa (23 °C < T < 42 °C)	E_f	129.5 GPa	E_m	2 GPa
E_{SMA}	83 GPa (57 °C < T < 75 °C)	ν_f	0.3	ν_m	0.3
ν_{SMA}	0.3	ρ_f	1750 kg/m^3	ρ_m	1200 kg/m^3
ρ_{SMA}	6450 kg/m^3				

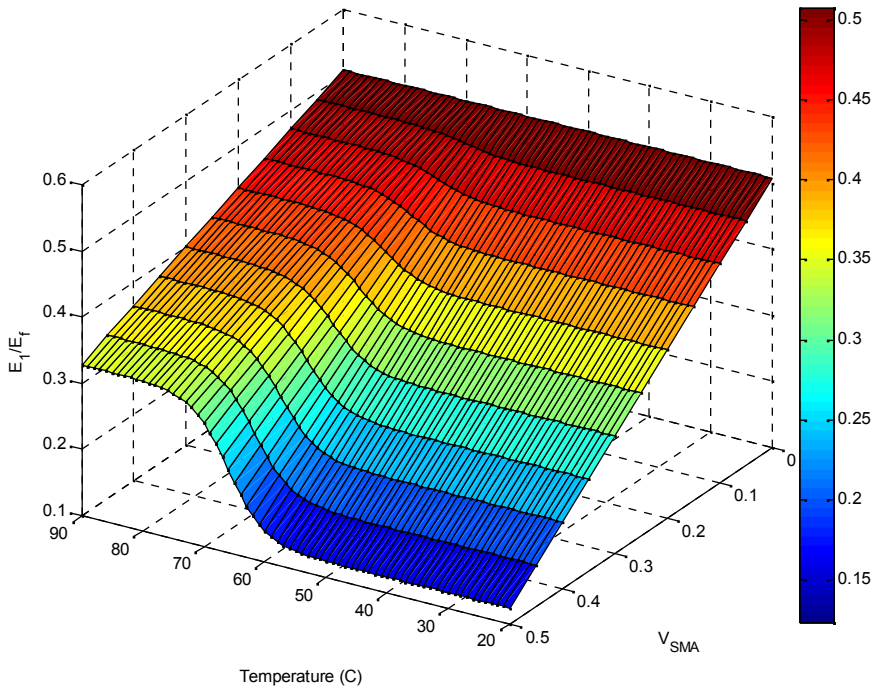

Figure 2 – Variation of the normalized modulus E_1/E_f with temperature and SMA volume fraction: A_S = 57 °C, A_F = 75 °C, β = 6.2.

AEROELASTIC PROBLEM

Figure 3 depicts the configuration studied and the cylindrical coordinate system used in the analysis. The shell is considered to be thin with total thickness h and adequately modeled by Kirchhoff's assumptions. A supersonic flow with airspeed U_∞ along x is imposed on the panel.

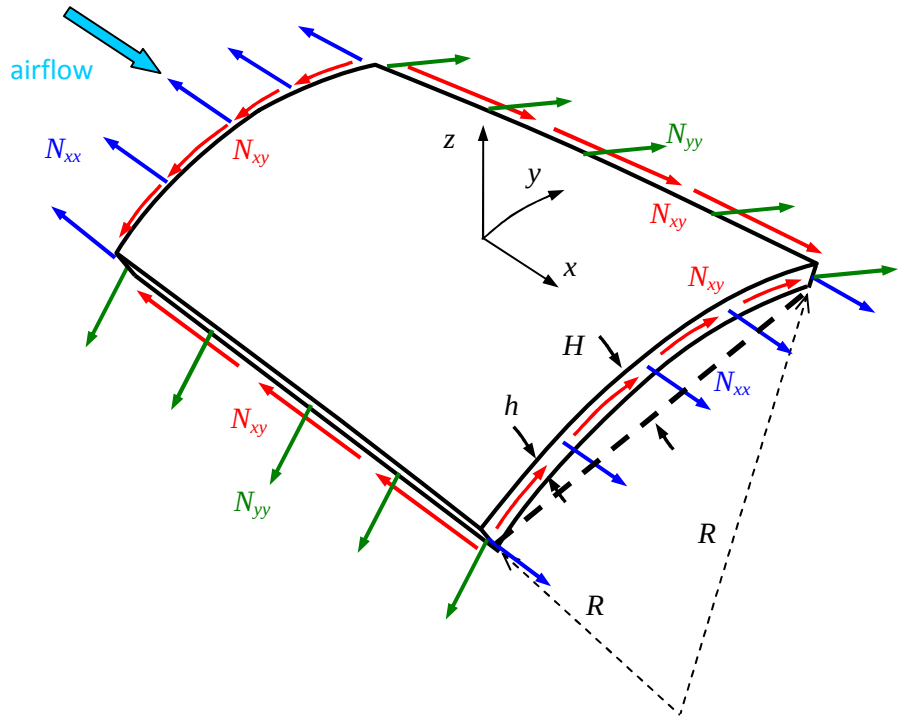

Figure 3 – Curved cylindrical panel in the presence of supersonic flow.

The cylindrical panel is modeled using classical thin-shell theory and von Kármán nonlinear strain × displacement relations. Accordingly, the in-plane displacements $\bar{u}(x,y,z)$ and $\bar{v}(x,y,z)$ are assumed to vary linearly through the thickness with respect to *z* and the transverse displacement $\bar{w}(x,y,z)$ is assumed independent of *z*. The dynamic differential equations are

$$\begin{aligned} &N_{xx,x} + N_{xy,y} = 0 \\ &N_{xy,x} + N_{yy,y} = 0 \\ &M_{xx,xx} + 2M_{xy,xy} + M_{yy,yy} + N_{0xx}w_{,xx} + 2N_{0xy}w_{,xy} + N_{0yy}w_{,yy} - \frac{N_{yy}}{R} + \lambda w_{,x} = \rho h\ddot{w} \end{aligned} \tag{8}$$

NUMERICAL SOLUTION

Assuming a symmetric laminate the dynamic equation in the transverse direction is

$$\begin{aligned} &D_{11}(\xi,T)w_{,xxxx} + 4D_{16}(\xi,T)w_{,xxxy} + 2[D_{12}(\xi,T) + 2D_{66}(\xi,T)]w_{,xxyy} + 4D_{26}(\xi,T)w_{,xyyy} + \\ &D_{22}(\xi,T)w_{,yyyy} - N_{0xx}w_{,xx} - 2N_{0xy}w_{,xy} - N_{0yy}w_{,yy} + N_{yy}/R - \lambda w_{,x} + \rho h\ddot{w} = 0 \end{aligned} \tag{9}$$

In order to solve Eq. (9), the Airy stress function *F* is defined as

$$N_{xx} = \frac{\partial^2 F}{\partial y^2} \qquad N_{yy} = \frac{\partial^2 F}{\partial x^2} \qquad N_{xy} = -\frac{\partial^2 F}{\partial x \partial y} \tag{10}$$

Considering the linearized membrane strains one can write the compatibility equation as

$$\begin{aligned} &A_{11}^{*}(\xi,T)F_{,yyyy} - 2A_{16}^{*}(\xi,T)F_{,xyyy} + [2A_{12}^{*}(\xi,T) + A_{66}^{*}(\xi,T)]F_{,xxyy} - 2A_{26}^{*}(\xi,T)F_{,xxxy} + \\ &A_{22}^{*}(\xi,T)F_{,xxxx} - w_{,xx}/R = 0 \end{aligned} \tag{11}$$

Solution of the dynamic governing equations, Eqs. (9) and (11), is achieved using the finite element method where

the Galerkin approach is used. Equation (9) is multiplied by δw, an arbitrary but kinematically admissible displacement satisfying the homogeneous geometric boundary conditions applicable to w, and later integrated over A. Similarly, Eq. (11) is multiplied by δF, an arbitrary variation satisfying the homogeneous geometric boundary conditions applicable to F, and later integrated over A.

The weak form of the resulting variational equations thereby obtained are discretized using the R16 element which has 4 nodes and 8 degrees of freedom per node: w, $w_{,x}$, $w_{,y}$, $w_{,xy}$, F, $F_{,x}$, $F_{,y}$ and $F_{,xy}$ (Bismarck-Nasr, 1999). Within each element both w and F are interpolated with the Hermitian polynomials. Usual assemblage of the element matrices leads to the global matrix equations

$$\begin{aligned} &\mathbf{M}\ddot{\mathbf{w}} + \mathbf{K}_{ww}(\xi,T)\mathbf{w} + \mathbf{K}_{wF}(\xi,T)\mathbf{f} + \lambda\mathbf{A}\mathbf{w} + [N_{0xx}\mathbf{K}_{Gxx} + N_{0yy}\mathbf{K}_{Gyy} + N_{0xy}\mathbf{K}_{Gxy}]\mathbf{w} = \mathbf{0} \\ &\mathbf{K}_{Fw}\mathbf{w} + \mathbf{K}_{FF}(\xi,T)\mathbf{f} = \mathbf{0} \end{aligned} \tag{12}$$

The degrees of freedom relative to F can be easily eliminated since $\mathbf{f} = -(\mathbf{K}_{FF}(\xi,T))^{-1}\mathbf{K}_{Fw}\mathbf{w}$ leading to

$$\mathbf{M}\ddot{\mathbf{w}} + [\mathbf{K}_{ww}(\xi,T)\mathbf{w} - \mathbf{K}_{wF}\mathbf{K}_{FF}^{-1}(\xi,T)\mathbf{K}_{Fw} + \lambda\mathbf{A} + N_{0xx}\mathbf{K}_{Gxx} + N_{0yy}\mathbf{K}_{Gyy} + N_{0xy}\mathbf{K}_{Gxy}]\mathbf{w} = \mathbf{0} \tag{13}$$

Assuming that vector w is of the form $\mathbf{w} = \mathbf{w}_0 \exp(j\omega t)$, where ω is the vibration frequency of the structure, $\mathbf{w}_0$ is the amplitude vector and $j = \sqrt{-1}$, Eq. (13) becomes

$$[-\omega^2\mathbf{M} + \mathbf{K}_{ww}(\xi,T)\mathbf{w} - \mathbf{K}_{wF}\mathbf{K}_{FF}^{-1}(\xi,T)\mathbf{K}_{Fw} + \lambda\mathbf{A} + N_{0xx}\mathbf{K}_{Gxx} + N_{0yy}\mathbf{K}_{Gyy} + N_{0xy}\mathbf{K}_{Gxy}]\mathbf{w}_0 = \mathbf{0} \tag{14}$$

MODE COALESCENCE

The point where the modal frequencies first coalesce indicates the beginning of the unstable flutter response. Thus, the critical aerodynamic pressure parameter λ_{cr} corresponds to the point where there occurs the first coalescence of modes and is therefore the aeroelastic flutter stability boundary or frontier. Figures 4 and 5 show coalescence of the principal vibration modes of a simply supported flat panel made of a 3 mm thick SMAHC single layer oriented at $\theta = 0^o$ with $a = b = 0.4$ m and $a/h = 100$ at two different temperatures. The mechanical properties of the constituents are presented in Table 1. Notice that, for this panel configuration, coalescence of the second and third modes occurs when the dynamic pressure parameter reaches $\lambda_{cr} = 5.4\times10^{-5}$ kg/ms^2 when the SMAHC is subjected to $T = 25$ ^{o}C and further increased to $\lambda_{cr} = 6.95\times10^{-5}$ kg/ms^2 at $T = 90$ ^{o}C, which clearly indicates that control of the occurrence of flutter speed can be achieved by controlling the temperature of the SMA wires. Similar behavior was also found for SMAHC single layers at different orientations, however for angle-ply laminates, the modes coalescence is highly dependent on the ply angle as shown in Figure 6. The numerical results indicate that, for panels with $a = b = 0.4$, the vibration modes of the flat panel are not affected by the boundary condition. Figure 7 depicts the first four predicted vibration modes of the SMAHC flat panel valid for panels subjected to clamped or simply supported boundary conditions along the edges.

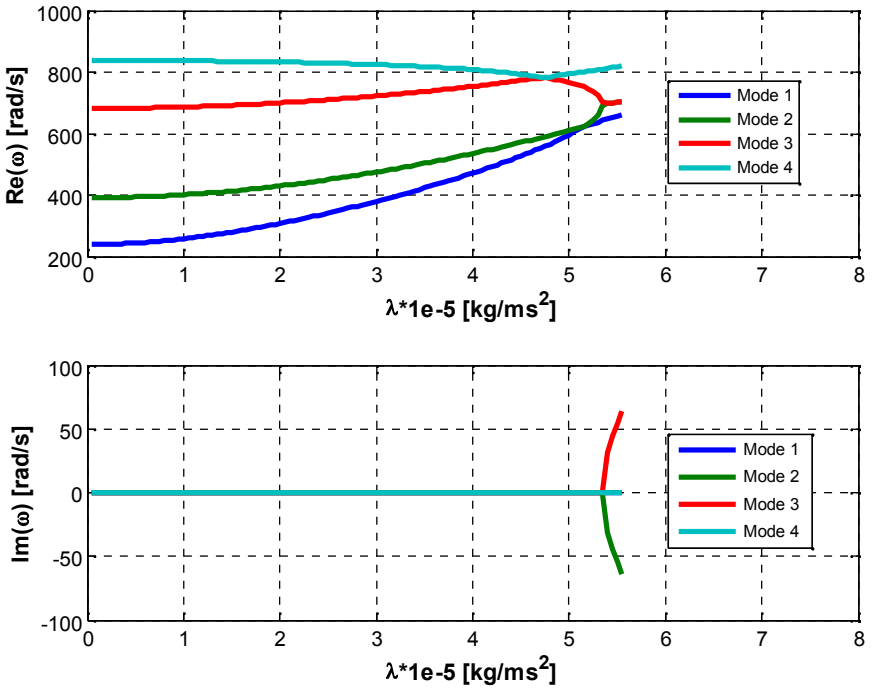

Figure 4 – Coalescence of the principal vibration modes for the SMAHC at T = 25 ^{o}C.

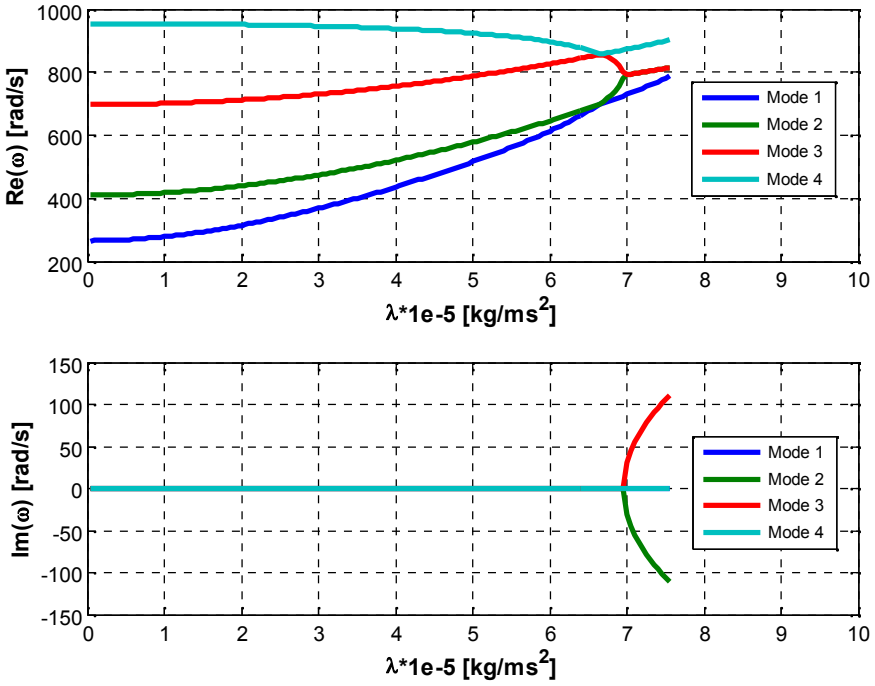

Figure 5 – Coalescence of the principal vibration modes for the SMAHC at T = 90 oC.

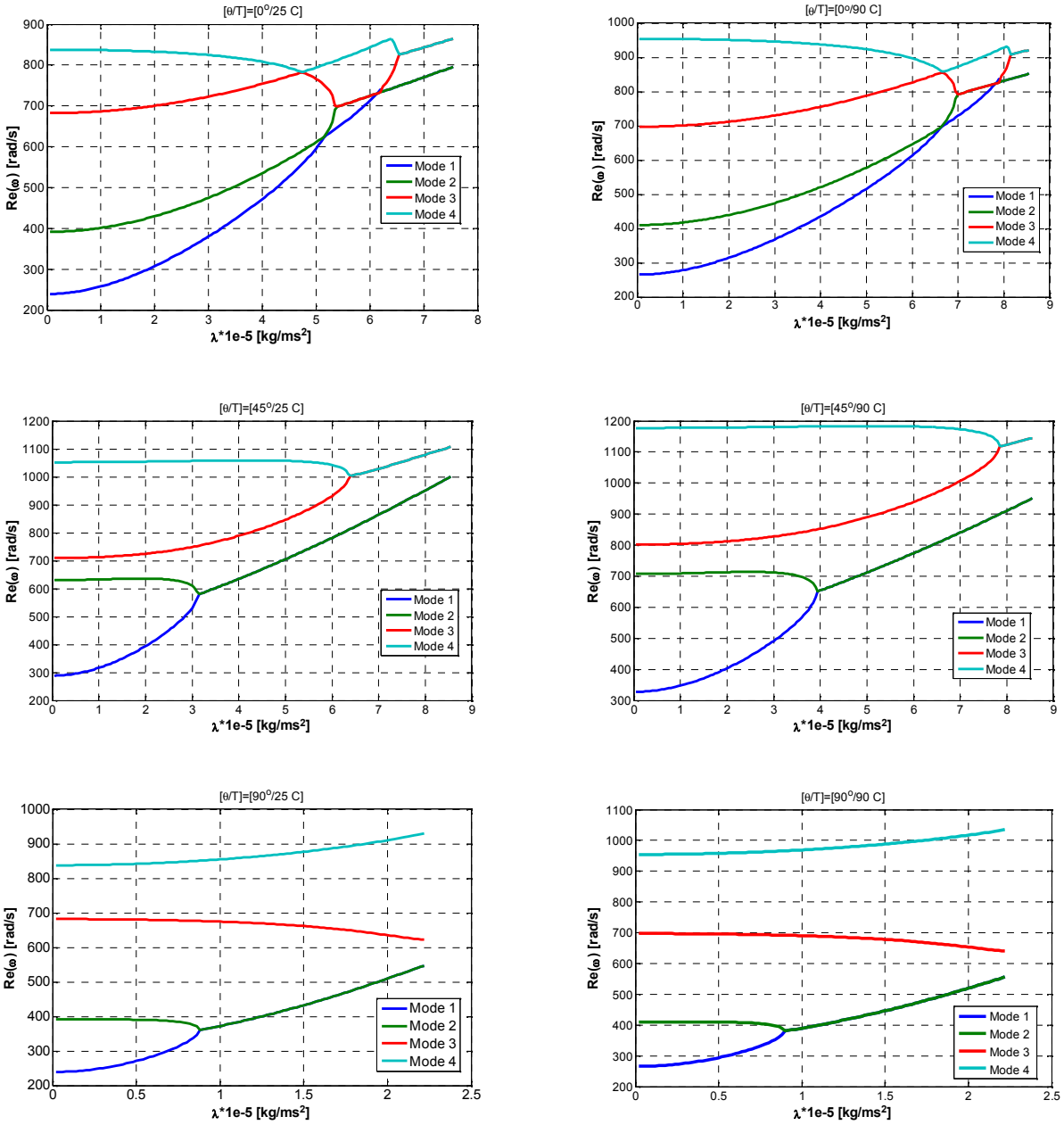

Figure 6 – Effects of the ply angle and temperature on the modes coalescence of a simply-supported SMAHC flat panel.

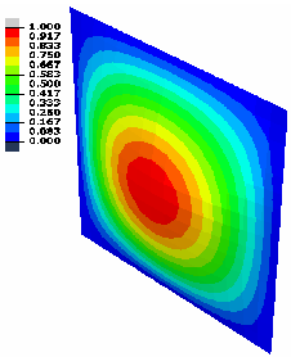

Mode 1

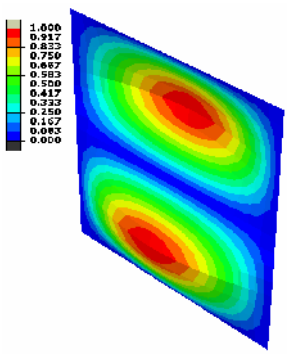

Mode 2

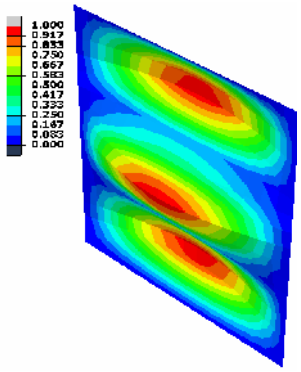

Mode 3

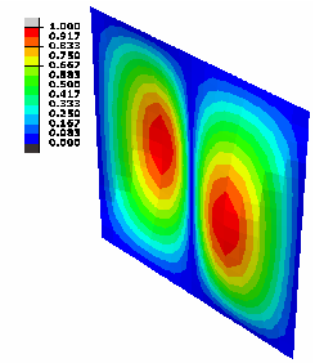

Mode 4

Figure 7 – four vibration modes of the SMAHC flat panel with *a* = *b* = 0.4 m.

CONCLUSIONS

The present paper presented a micromechanical model for composite laminates reinforced by carbon fiber and shape memory allow wires. The micromodel accounts for the stiffening effects induced by the SMA phases transformation and allows adjustment of different reinforcement volume fractions. The formulation can be easily extended for multi-constituent composites. The proposed micromodel was incorporated into a finite element formulation for flutter prediction in Shape Memory Alloy Hybrid Composite (SMAHC) panels. Numerical simulations were carried out for SMAHC panels with different layups, geometries and boundary conditions. The numerical predictions clearly indicate that control of the occurrence of flutter speed can be achieved by controlling the temperature of the SMA wires in the SMAHC laminates. The assessment conducted pointed to a large array of parameter combinations that may yield the best conditions for flutter aeroelastic instability control using Shape Memory Alloys in aeronautical panels.

The highest effectiveness is observed for panels with aspect ratios near unity. This means that, in practice, it is advisable to subdivide long panels into nearly square subpanels by the use of reinforcements. Long rectangular panels should then be subdivided using one or more reinforcements running parallel to its shortest edges.

ACKNOWLEDGMENTS

This work was partially funded by the Brazilian Agency CNPq through Grants 300990/2013-8 and 300886/2013-6.

REFERENCES

de Faria A.R., Almeida, S.F.M, 1996, Modeling of actively damped beams with piezoelectric actuators with finite stiffness bond, Journal of Intelligent Material Systems and Structures, Vol. 7, pp. 677-688.

Parka, J.-S., Kima, J.-H. and Moonb, S.-H., 2005, Thermal post-buckling and flutter characteristics of composite plates embedded with shape memory alloy fibers, Composites Part B: Engineering, Vol. 36, pp. 627-636.

Guo, X., Lee, Y.-Y. and Mei, C., 2007, Supersonic nonlinear panel flutter suppression using shape memory alloys, Journal of Aircraft, Vol. 44, pp. 1139-1149.

Ibrahim, H.H., Yoo, H.H. and Lee, K.-S., 2009, Thermal buckling and flutter behavior of shape memory alloy hybrid composite shells, Journal of Aircraft, Vol. 46, pp. 895-902.

Kuo, S.-Y., Shiau, L.-C. and Lai, C.-H., 2012, Flutter of buckled shape memory alloy reinforced laminates, Smart Materials and Structures, Vol. 21, pp. 1-10.

Bismarck-Nasr, M.N., 1991, On the sixteen degree of freedom rectangular plate element, Computer and Structures, Vol. 40, pp. 1059-60.

Kaw, A.K., 2006, Mechanics of Composite Materials, CRC Taylor & Francis, second ed., Boca Raton

Aquino, S.A., Borges, J.M., Silva Irmão, M.A. and Silva, A.A., 2010, Controle de vibrações mecânicas utilizando propriedades das ligas com memória de forma. Proceedings of the VI National Congress of Mechanical Engineering, Campina Grande-Paraíba, Brazil.

Bismarck-Nasr, M.N., 1999, Structural dynamics in aeronautical engineering. Reston, AIAA Education Series.

RESPONSIBILITY NOTICE

The authors are the only responsible for the material included in this paper.